Nuclear pore complex proteins mark the implantation window in human endometrium

Elisa Guffanti[1], Nupur Kittur[1], Z. Nilly Brodt[1], Alex J. Polotsky[2], Satu M. Kuokkanen[2], Debra S. Heller[3], Steven L. Young[4], Nanette Santoro[2] and U. Thomas Meier[1,*]

[1]Department of Anatomy and Structural Biology and [2]Department of Obstetrics, Gynecology and Women's Health, Albert Einstein College of Medicine, 1300 Morris Park Avenue, Bronx, NY 10461, USA
[3]Department of Pathology, UMDNJ – New Jersey Medical School, Newark, NJ 07101, USA
[4]Department of Obstetrics and Gynecology, University of North Carolina School of Medicine, Chapel Hill, NC 27599, USA
*Author for correspondence (e-mail: meier@aecom.yu.edu)

Accepted 3 April 2008
Journal of Cell Science 121, 2037-2045 Published by The Company of Biologists 2008
doi:10.1242/jcs.030437

Summary

Nucleolar channel systems (NCSs) are membranous organelles appearing transiently in the epithelial cell nuclei of postovulatory human endometrium. Their characterization and use as markers for a healthy receptive endometrium have been limited because they are only identifiable by electron microscopy. Here we describe the light microscopic detection of NCSs using immunofluorescence. Specifically, the monoclonal nuclear pore complex antibody 414 shows that NCSs are present in about half of all human endometrial epithelial cells but not in any other cell type, tissue or species. Most nuclei contain only a single NCS of uniform 1 μm diameter indicating a tightly controlled organelle. The composition of NCSs is as unique as their structure; they contain only a subset each of the proteins of nuclear pore complexes, inner nuclear membrane, nuclear lamina and endoplasmic reticulum. Validation of our robust NCS detection method on 95 endometrial biopsies defines a 6-day window, days 19-24 (±1) of an idealized 28 day cycle, wherein NCSs occur. Therefore, NCSs precede and overlap with the implantation window and serve as potential markers of uterine receptivity. The immunodetection assay, combined with the hitherto underappreciated prevalence of NCSs, now enables simple screening and further molecular and functional dissection.

Key words: Human reproduction, Nuclear envelope, Nuclear organelle

Introduction

During an idealized 28-day human menstrual cycle, the endometrium undergoes well-timed changes in preparation for embryo implantation. The follicular or proliferative phase is separated by ovulation on day 14 from the luteal or secretory phase. The endometrium is only receptive to embryo implantation during luteal days 20-24 (Wilcox et al., 1999). Inability to determine endometrial receptivity is one important cause for less than optimal success rates in artificial reproductive technologies such as in vitro fertilization (Norwitz et al., 2001).

These temporal changes of the endometrium are evident at the tissue and epithelial cell level. In fact, histological changes have been the gold standard for endometrial dating for the past 50 years, but their value has recently been questioned (Coutifaris et al., 2004; Murray et al., 2004; Noyes et al., 1950). Among the ultrastructural hallmarks of secretory endometrial epithelial cells are giant mitochondria, subnuclear glycogen deposits, pinopodes and nucleolar channel systems (NCSs) (Martel, 1981; Spornitz, 1992). Whereas giant mitochondria and subnuclear glycogen deposits appear in the early luteal phase, pinopodes (see Discussion) and NCSs more closely overlap with the mid-luteal window of implantation and could serve as potential markers (Clyman, 1963; Nikas et al., 1995).

NCSs were discovered close to 50 years ago in the nuclei of endometrial epithelial cells using transmission electron microscopy, which is currently their only method of identification (Dubrauszky and Pohlmann, 1960). NCSs are small globular structures of about 1 μm in diameter and consist of three components: intertwined membrane tubules embedded in an electron-dense matrix, and an amorphous core that is separated from the nucleoplasm by the tubules and matrix (Clyman, 1963; Moricard and Moricard, 1964; Terzakis, 1965). Using histochemical labeling, we documented the activity of glucose-6-phosphatase, a marker enzyme of endoplasmic reticulum, in the lumen of the membrane tubules, indicating their derivation from this cytoplasmic organelle, apparently through the contiguous nuclear envelope (Kittur et al., 2007).

Our understanding of nuclear structure and function has advanced significantly (Stewart et al., 2007; Terry et al., 2007; Trinkle-Mulcahy and Lamond, 2007). Nuclear pore complexes (NPCs) perforate the nuclear envelope at the sites where the outer and inner nuclear membranes fuse and are thought to serve as the sole portals between nucleus and cytoplasm. The NPCs are large protein assemblies consisting of 30 or so proteins (nucleoporins) present in multiple copies and arranged in partial symmetry across the envelope and around the pore. Although some nucleoporins can transiently detach from NPCs during interphase and some concentrate in kinetochores during mitosis when NPCs disassemble, they are generally restricted to intact NPCs (Belgareh et al., 2001; Rabut et al., 2004). Whereas the outer membrane and the perinuclear space mirror the proteins of the attached endoplasmic reticulum, the protein composition of the inner nuclear membrane is distinct. Inner membrane proteins anchor the lamina (an intermediate filament meshwork lining the nucleoplasmic side) and/or chromatin at the nuclear envelope. Several of these proteins, including lamins (proteins of the lamina), are mutated in inherited diseases ranging from muscular dystrophies to progeria (premature aging) (Stewart

et al., 2007). Here we document the unprecedented congregation of only some of these nucleoporins, inner membrane and lamin proteins in NCSs, furthering the mystery of these membranous organelles in the normally membrane-free nucleus.

Several lines of evidence suggest a role for NCSs in the preparation of the endometrium for reception of the embryo. NCSs have strictly been observed post ovulation, only on cycle days 16-24, and are not detected in pregnancy (Clyman, 1963). They appear to be induced by progesterone and are sensitive to oral and intrauterine contraceptives (Azadian-Boulanger et al., 1976; Feria-Velasco et al., 1972; Kohorn et al., 1970; Kohorn et al., 1972; Pryse-Davies et al., 1979; Roberts et al., 1975; Wynn, 1967). Finally, in several cases of unexplained infertility the absence or delayed appearance of NCSs was noted as the sole abnormal endometrial parameter (Dockery et al., 1996; Gore and Gordon, 1974; Kohorn et al., 1972). Despite this and additional evidence, NCSs have been neglected as potential markers or prerequisites for implantation. This can be mostly attributed to the difficulty of their detection, which requires transmission electron microscopy and is compounded by their small size and the perception that only about 5% of all endometrial epithelial cells develop NCSs (Novotny et al., 1999; Ryder et al., 1995). Here we describe the first light microscopic detection and molecular dissection of NCSs, which are about ten times more abundant than previously appreciated and mark the window of uterine receptivity.

Results

Light microscopic detection of NCSs

In electron micrographs, NCSs are often associated with the nuclear envelope. Therefore, we tested for the presence in NCSs of proteins from the nuclear boundary using indirect immunofluorescence on semi-thin frozen sections of human endometrium. Indeed, the monoclonal antibody 414 (mAb414), directed against a subset of nuclear pore complex proteins (Davis and Blobel, 1986), identified rings in the nuclei of some endometrial epithelial cells (Fig. 1A, arrows). Although sometimes associated with nucleoli (Fig. 1A', arrowheads), these structures were distinct entities and had a darker ring-shaped appearance in phase-contrast images of these 0.5-μm-thick sections (Fig. 1A', arrows). Nevertheless, similarly to nucleoli, these rings did not stain for DNA (Fig. 1A''). The concentration of nucleoporins in these structures proved so high that the classical punctate NPC staining of the nuclear periphery only became evident upon overexposure of the same image (Fig. 1A'''). To determine the identity of these structures on an ultrastructural level, cryosections of human endometrium were stained with mAb414 followed by gold-labeled secondary antibodies. In addition to a NPC in an adjacent cell nucleus, mAb414 specifically, and to a high-density, labeled NCSs but not adjacent nucleoli or other cellular compartments (Fig. 1B). Therefore, the rings identified at the light microscopic level were NCSs rendering mAb414 a specific marker for this nuclear organelle. The additional labeling of NPCs serves as a control for positive antibody staining and demarcation of cell nuclei.

To test the robustness of the mAb414 staining method and its applicability to more commonly available paraffin-embedded tissue, paraffin sections of human endometrium were labeled. As in cryosections, mAb414 specifically stained NCSs and NPCs of epithelial cell nuclei whether visualized by epifluorescence (Fig. 2I) or confocal fluorescence microscopy (Fig. 1C).

NCSs are abundant organelles specific to human endometrial epithelial cells

In single 0.5-μm-thick cryosections or 0.2-μm-thick optical confocal planes of paraffin sections, NCSs are observed in only about 10% of epithelial cell nuclei (Fig. 1C), although clusters of NCS-positive nuclei can be observed (Fig. 1A). To assess the number of NCSs in entire nuclei, 7-μm-thick paraffin sections were stained with mAb414 and imaged across their entire thickness in 0.2 μm steps using confocal laser-scanning microscopy. Whereas a NCS is visible in only one nucleus of a single optical plane (Fig. 1C), NCSs are detected in most nuclei of a maximum projection of all planes (Fig. 1C'). Analysis in this manner of 237-1305 epithelial cell nuclei per endometrial biopsy from 11 women (Fig. 4A, black dots) revealed the following facts about NCSs (Table 1). In total, 6951 nuclei contained 3175 NCSs corresponding to 46% of epithelial cell nuclei. In individual women, the number of NCSs varied

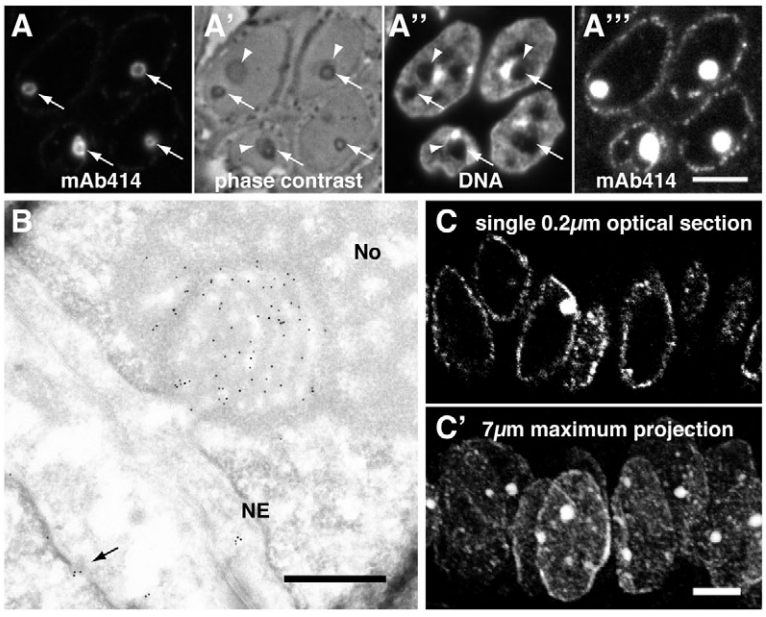

Fig. 1. The monoclonal antibody 414 (mAb414) directed against nuclear pore complex (NPC) proteins exhibits a strong preference for NCSs. (A) Double fluorescence of mAb414 (A) and DAPI DNA stain (A'') on a semi-thin frozen section of human endometrium in the secretory phase. NCS fluorescence appears as rings (A, arrows). The rings, i.e. the matrix and membrane tubules of NCSs, appear as phase-dense circles in phase contrast microscopy (A', arrows). Moreover, NCSs are often encircled by nucleoli (arrowheads) and, like nucleoli, appear chromatin-free (A''). The concentration of mAb414 antigens in NCSs is so high that the classical rim staining of NPCs only becomes visible if the image is overexposed to an extent that saturates NCS staining (A'''). (B) MAb414 immunogold-stained electron micrograph of an ultrathin cryosection of luteal human endometrium. Note the strong and specific gold labeling of a grazing section of a NCS (i.e. its core is covered by its membrane tubules and matrix) that is embedded in a nucleolus (No) and attached to the nuclear envelope (NE). At least one NPC of a neighboring cell is identified by mAb414 (arrow). (C) Confocal micrograph of indirect mAb414 fluorescence of a 7-μm-thick paraffin section of luteal human endometrium. In a single 0.2 μm optical section, a NCS is visible in only one of the nuclei defined by the classical rim staining of NPCs (C), whereas, in a maximum projection of all optical planes, all nuclei outlined by hazy NPC staining contain NCSs (C'). Scale bars: 5 μm.

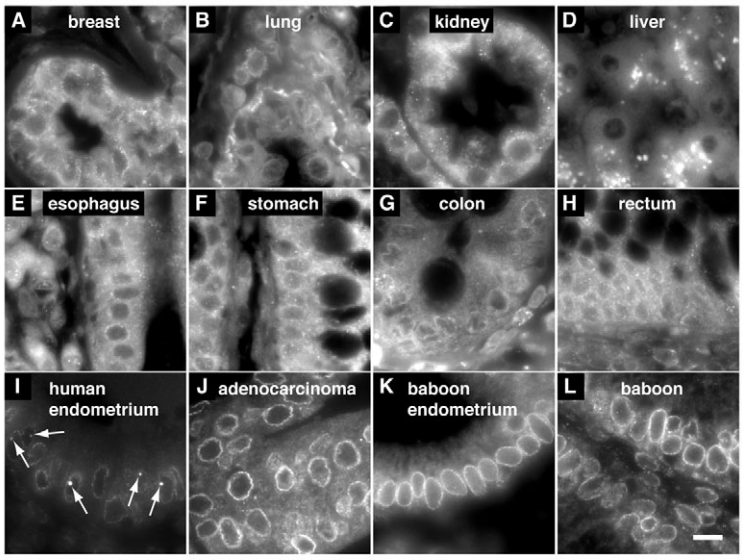

Fig. 2. NCSs are specific to human endometrium. Indirect mAb414 fluorescence on paraffin sections of various human (A-J) and baboon tissues (K,L). (A-J) Samples from commercial tissue arrays. One example out of six specimens each of human breast (A), lung (B), kidney (C), liver (D), esophagus (E), stomach (F), colon (G), and rectum (H) tissue. One example out of 59 specimens each of human control endometrium (I) and endometria with adenocarcinomas (J). (K,L) Two examples out of 19 baboon secretory endometrial biopsies. Note only control human secretory endometrium contains NCSs (arrows). Nuclear pore complex staining is generally better in endometria but, despite high background labeling, can be distinguished in the other tissues and should therefore reveal NCSs if present. Scale bar: 10 μm.

between 27% and 58% with an average of 44±9% (Table 1). Most nuclei contained only a single NCS, although two and, in rare cases, up to five, were also observed. All NCSs were apposed to the nuclear envelope and the largest and most abundant NCSs were uniform in size with a diameter of 1 μm. This overall abundance and limitation in number per nucleus and size suggests a physiological role and a tight regulation of NCSs in the postovulatory endometrium.

NCSs were most abundant in epithelial glands but also present in luminal epithelium facing the uterine cavity. However, on no occasion were NCSs observed in nuclei of stromal cells (e.g. Fig. 2I and Fig. 4B). Moreover, analysis of tissue arrays containing six paraffin sections each of human esophagus, stomach, liver, colon, rectum, lung, kidney and breast tissue, failed to reveal any NCSs when stained with mAb414 (Fig. 2A-H). This is most remarkable for breast tissue, which, like endometrium, is under control of ovarian hormones. When endometrial tissue arrays from healthy and carcinoma patients were stained, 17% (n=59) of control specimens contained NCSs (which is in the expected range if biopsies were taken randomly throughout the cycle), whereas none of the carcinoma sections showed any (Fig. 2I and J, respectively). Therefore, NCSs are restricted to the nuclei of healthy endometrial epithelial cells.

Table 1. Quantitative analysis of NCSs by confocal microscopy

Biopsy ID*	Luteal day†	Epithelial cells counted	% with NCSs
85	4	272	36
78	4	1305	55
5	4	380	47
36	5	973	42
10	6	237	41
97	8	830	54
25	9	687	45
67	9	415	58
57	10	448	27
28	11	370	42
54	11	1034	40
Total		6951	44 (±9)‡

*Endometrial biopsies analyzed are marked in Fig. 4A (black dots).
†Day biopsy was collected.
‡Mean ± s.d.

Reportedly, NCSs are absent from animal endometria, even those of baboons (Clyman, 1963; MacLennan et al., 1971). To re-evaluate this information with our robust NCS detection method, we analyzed endometrial paraffin sections from 19 baboons collected during the height of receptivity. Although the NPCs were readily detected by mAb414, no NCSs were identified (Fig. 2K,L). Hence, the NCS is a human-specific organelle.

The NCS is an organelle of unique composition

In a candidate approach, we used colocalization with mAb414 for an initial compositional analysis of NCSs. First, we investigated whether all nucleoporins recognized by mAb414 were present, because, on an ultrastructural level, no intact NPCs can be distinguished within NCSs. Indeed, when using nucleoporin-specific antibodies, only Nup153 and Nup62, but not Nup358 or Nup214 were present in NCSs (Fig. 3A-D). Whereas the latter mark the cytosolic face of NPCs, the former constitute part of the central and nucleoplasmic face of NPCs (Tran and Wente, 2006). Therefore, we tested for the presence of translocated promoter region (Tpr), a nucleoporin interacting with Nup153 and forming the nuclear baskets of NPCs (Hase and Cordes, 2003; Krull et al., 2004). Interestingly, Tpr was enriched in some, mostly full-sized, NCSs but absent from others (Fig. 3F, compare arrow and arrowheads). This indicates the existence of two classes of NCSs that differ in composition and/or developmental stages, i.e. an early stage without and a mature one with Tpr, possibly mirroring the late recruitment of Tpr to NPCs in telophase (Hase and Cordes, 2003). Many nucleoporins, including Nup153 and Nup62, are post-translationally modified by single O-linked N-acetylglucosamine moieties, which bind the lectin wheat germ agglutinin (Davis and Blobel, 1986; Davis and Blobel, 1987). This lectin indeed recognized NCSs, presumably binding the sugar moieties of Nup153 and Nup62, which consequently must have been modified like their counterparts in NPCs (Fig. 3E). NPCs are anchored in the intermediate filament meshwork of the nuclear lamina that spans the inner nuclear envelope. Although lamins A/C were highly enriched in NCSs (Fig. 3I,J'), lamin B1 was barely detectable (Fig. 2H), whereas B2 was

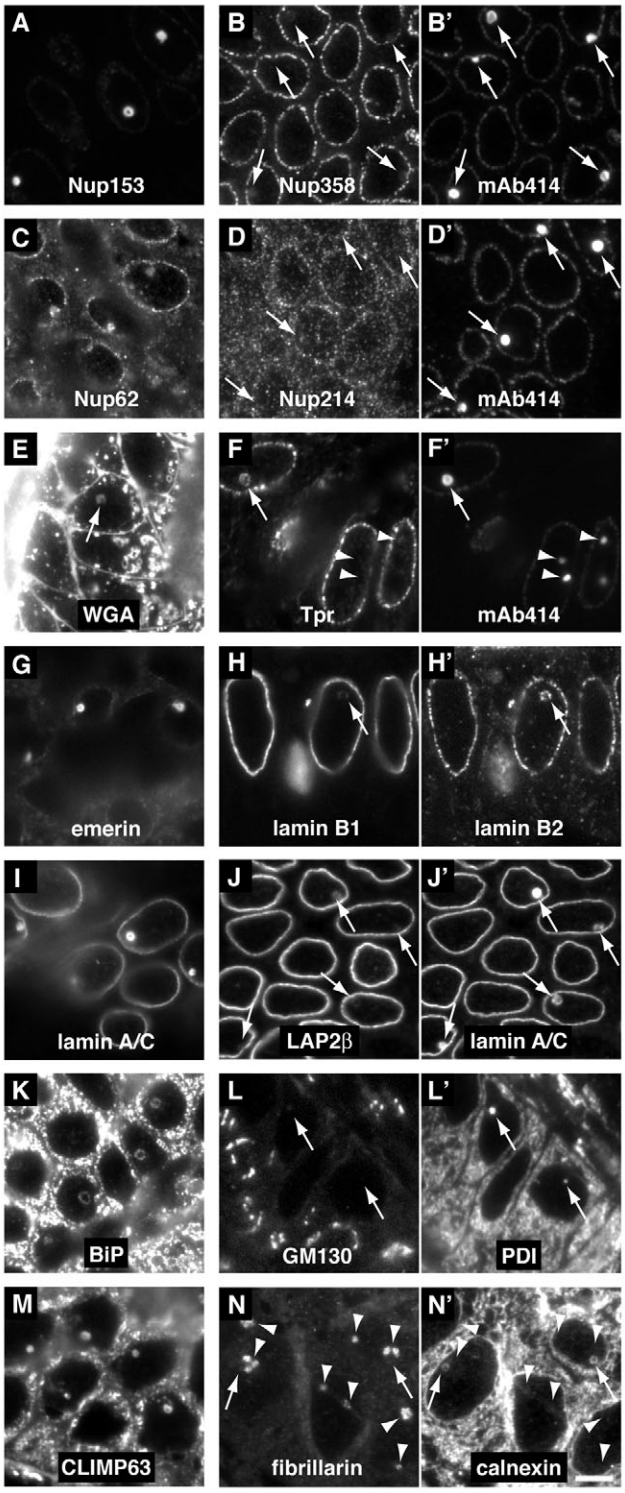

Fig. 3. NCSs consist of a unique subset of NPC, and nuclear membrane and lamina proteins. Indirect immunofluorescence on semi-thin frozen sections of human luteal endometrium of antigens clearly present and/or enriched in NCSs (left column: A,C,E,G,I,K,M), of antigens absent from, barely detectable, or only in some NCSs (middle column: B,D,F,H,J,L,N), and of antigens clearly present in NCSs as double fluorescence control (right column: B',D',F',H',J',L',N'). The identity of all antigens is indicated on each panel. NCSs that are not obvious (E) and all in the double fluorescence series (two right columns) are indicated (arrows). In all cases, the identity of NCSs was confirmed by double fluorescence and/or phase-contrast microscopy. Note that although mAb414 recognizes all four nucleoporins, only Nup153 (A) and Nup62 (C) but not Nup358 (B) nor Nup214 (D) are present in NCSs. Tpr is present in only some (F, arrow) but not other NCSs (arrowheads). Of the two inner nuclear membrane and lamina-associated proteins emerin (G) and LAP2β (J), only emerin is enriched in NCSs. Nucleoli, identified by fibrillarin (N, arrowheads), are often adjacent to or surrounding NCSs (N', arrows) but do not overlap. Note the particularly high enrichment in NCSs of Nup153 (A), emerin (G) and lamin A/C (I), which at this exposure are barely detectable in their usual nuclear envelope locations. Magnification is identical in all panels; scale bar, 5 μm.

present (Fig. 2H'). Of two integral membrane proteins specific to the inner nuclear membrane, emerin was most highly enriched in NCSs (Fig. 2G), whereas LAP2β was barely, if at all, detectable (Fig. 2J). This was surprising because both proteins belong to the lamin-interacting LEM-domain proteins (Lin et al., 2000; Wagner and Krohne, 2007). Unprecedented therefore, NCSs are composed of a specific subset of nuclear envelope proteins, part NPC, part lamina and part inner membrane.

Apparently, the membrane tubules of the NCS are derived from the inner nuclear membrane, which is contiguous with that of the endoplasmic reticulum via the pore and the outer nuclear membrane. Therefore, we tested for the presence of endoplasmic reticulum proteins in NCSs. Both luminal, e.g. BiP and PDI, and integral membrane proteins, e.g. calnexin, could be detected in NCSs (Fig. 3K,L',N'). Surprisingly, even the cytoskeleton linking integral membrane protein CLIMP63, which is concentrated in the endoplasmic reticulum but absent from the nuclear envelope (Klopfenstein et al., 2001), was prominent in NCSs (Fig. 3M). However, the rough endoplasmic reticulum marker protein Sec61, which is part of the protein-conducting channel, was not detected (Table 2). Similarly, antigens further along the secretory pathway, e.g. from the Golgi apparatus, were absent from NCSs, specifically, GM130 and p115 (Fig. 3L and Table 2). Therefore, the NCS membrane system appears to derive from the nuclear envelope and the smooth endoplasmic reticulum.

As reflected in their name, NCSs are often surrounded by nucleoli in electron micrographs. A thorough analysis using three-dimensional confocal colocalization of mAb414 with the nucleolar marker Nopp140, which is not enriched in NCSs (Kittur et al., 2007), revealed 44% of NCSs (n=295) associated with nucleoli. Although only analyzed in 0.5-μm-thick frozen sections, there appeared to be an inverse relationship between the presence of Tpr in NCSs and their nucleolar association. To test whether a common composition, as in the case of other nuclear membrane structures (Isaac et al., 2001; Kittur et al., 2007), was responsible for this association, additional nucleolar proteins were investigated for their presence in NCSs. Surprisingly, nucleolar proteins never concentrated in NCSs but often were apposed to them in nucleoli (Fig. 3N and Table 2). Therefore, the molecular basis of the NCS-nucleolus relationship remains to be elucidated. Finally, none of the markers for other nucleoplasmic domains or functions accumulated in NCSs, specifically, the Cajal body marker coilin, the nuclear-speckle-specific splicing factor SC35, initiating or elongating RNA polymerase II or the progesterone and estrogen receptor transcription factors (Table 2). Consequently, the NCS represents a nuclear organelle of distinct composition.

The NCS marks the implantation window

Although previous electron microscopic studies agree that the NCS marks the postovulatory endometrium, the exact window of NCS appearance varies. Therefore, we tested our robust NCS detection

Table 2. List of antigens tested for presence in NCSs

Compartment	Antigen	in NCS
NPC	Nup153	+++*
	Nup62	+
	Nup358	–
	Nup214	–
	Tpr	+/–
	WGA	+
Nuclear envelope	Lamin A/C	+++
	Lamin A	+
	Lamin B1	(+)
	Lamin B2	+
	Emerin	+++
	LAP2β	(+)
Endoplasmic reticulum	Calnexin	+
	BiP	+
	PDI	+
	CLIMP63	+
	Sec61	–
Nucleolus	Nopp140	–
	NAP57/dyskerin	–
	Fibrillarin	–
	Nucleolin	–
	UBF1	–
Nucleoplasm	Coilin	–
	Pol II CTD S2-P†	–
	Pol II CTD S5-P‡	–
	SC35	–
	Progesterone receptor	–
	Estrogen receptor	–
Golgi	p115	–
	GM130	–

*+++, highly enriched; +, present; +/–, only in some; (+), barely detectable; –, absent.

†Antibodies specific for the phosphorylated Ser2 of the C-terminal domain of RNA polymerase II, which is characteristic for the initiating enzyme.

‡Antibodies specific for the phosphorylated Ser5 of the C-terminal domain of RNA polymerase II, which is characteristic for the elongating enzyme.

method on 95 endometrial biopsies from fertile women, 31 from the follicular and 64 from the luteal phase. NCSs were restricted to luteal days LH+4 to LH+13 and none were detected in any of the follicular phase biopsies (Fig. 4A,B). No NCSs were observed before day LH+4; after day LH+9 the number of NCSs appeared to gradually decline and the number of cells with few and no NCSs increased. Biopsies collected at two separate sites defined the same NCS window (Fig. 4A, black and white bars). This supports the general applicability of our methodology. Several biopsies had factors associated that could influence accurate dating (Fig. 4A, lettered biopsies). If all those biopsies were disregarded, NCSs were only observed in the window of days LH+4 to LH+10, except for a few NCSs in a day LH+13 biopsy. When considering all biopsies, over 70% of biopsies/day in that LH+4 to LH+10 window contained NCSs, whereas thereafter their number dropped to 50% and below (Fig. 4C). Interestingly, the fact that a patient under a regimen of high estrogen and low progesterone showed no NCSs on luteal day 7 (Fig. 4A, biopsy b) supports the requirement of progesterone for NCS induction. In summary, the appearance of NCSs peaks on cycle days LH+5 to LH+10 (±1 day), i.e. days 19-24 (±1) of an idealized 28-day cycle define the NCS window.

Discussion

The major impact of our results is twofold: the NCS detection assay provides a simple method for endometrial dating, and the unique molecular composition of the NCS provides a basis for understanding complex interactions governing nuclear architecture. Therefore, our discovery will be of interest to such diverse groups as practicing gynecologists and basic cell biologists.

Markers for uterine receptivity

Our identification of the first molecular markers of NCSs allowed development of a light microscopic assay for their detection. Application of this assay reveals a peak presence of NCSs in over 50% of endometrial epithelial cells or a tenfold higher prevalence than was appreciated based on previous electron microscopic

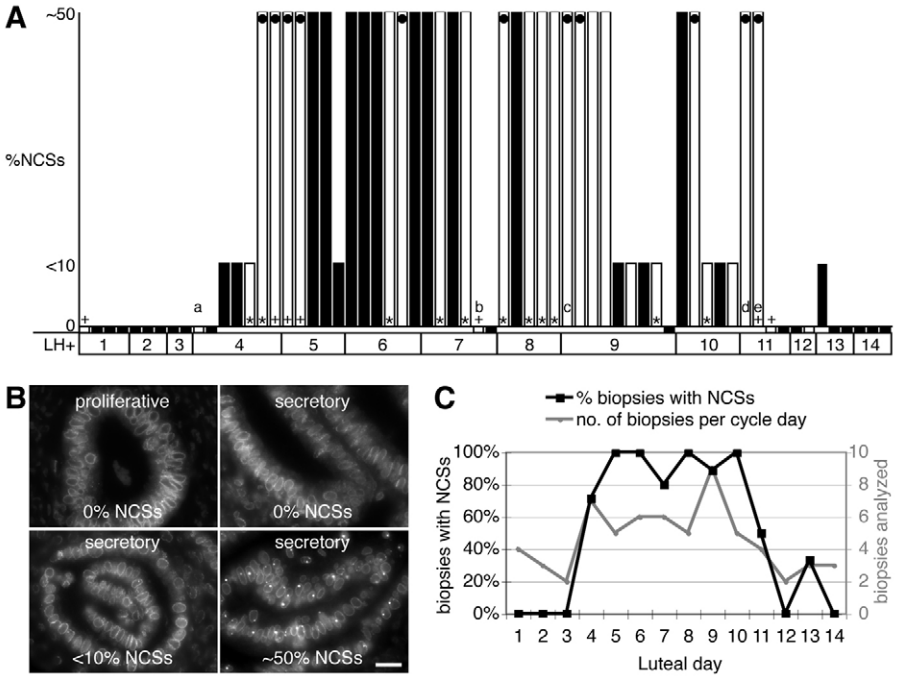

Fig. 4. The NCS marks the implantation window. (A) Histogram of 64 human endometrial biopsies collected on the indicated luteal days (LH+) and scored for the percentage of epithelial cell nuclei containing NCSs using three categories, none (0%), less than 10% (<10%), and between 10% and 60% but mostly around 50% (~50%). Where available, the luteal day was determined in the following order of priority, according to LH surge, classical histological criteria (+) (Noyes et al., 1950), and chronological day (*). Some biopsies from conditions that may affect dating are indicated: (a) fibroid uterus; (b) menopause transition treated with hyper estrogen and hypo progesterone; (c) 30-34 day cycle; (d) 34-37 day cycle; (e) dysmenorrhea. The biopsies in which NCSs were quantified more accurately (Table 1) are marked (black dots). (B) Representative mAb414 fluorescence micrographs for each category in (A) including a proliferative biopsy. Scale bar: 20 µm. (C) Summary of the data in A expressed as a percentage of biopsies on each luteal day containing NCSs (black squares, left *y*-axis) and the number of biopsies analyzed on each day (gray circles, right *y*-axis). Note that only on luteal days 4-10 did over 70% of biopsies contain NCSs.

studies (Novotny et al., 1999; Ryder et al., 1995). Therefore, our results establish the NCS as a major physiological hallmark of the postovulatory endometrium. Based on the analysis of 95 endometrial biopsies, NCSs define a six-day window, days 19-24 (±1) of an idealized 28-day cycle, which precedes and overlaps with the implantation window. Of course, the accuracy of this NCS window relative to the menstrual cycle depends on the accuracy of the endometrial dating. In this context, it should be noted that results from the dating methods that are commonly used, including in this study, can differ significantly (Murray et al., 2004). Nevertheless, NCS appearance can now be easily and reliably determined in fresh and archival endometrial biopsies using a robust immunodetection method.

Definition of the receptive period – the implantation window – of human endometrium remains a major challenge. This becomes particularly evident in artificial reproductive technologies that probably depend both on accurate timing and on ability to detect defects in receptivity to increase the low average implantation rate of ~25% (de los Santos et al., 2003). Long-standing histological markers of uterine receptivity are slowly giving way to molecular markers, although no single marker has been able to withstand the test of time (Aghajanova et al., 2007). With the development of our assay, the NCS combines a histological marker with molecular detection. NCSs may be a hallmark of receptive endometrium because they define a luteal window that closely mirrors serum progesterone levels. By contrast, pinopodes – apical membrane protrusions thought to be critical for and present at the site of blastocyst attachment – persist through early menses and pregnancy (Acosta et al., 2000; Bentin-Ley et al., 1999; Nikas et al., 1995; Usadi et al., 2003). Additionally, the value of pinopodes as implantation markers has recently been questioned (Petersen et al., 2005; Quinn et al., 2007). Here, we propose the long known, but mostly forgotten NCS as a marker for uterine receptivity.

Nuclear organelles of novel composition

The monoclonal antibody 414 is an excellent marker for NCSs. However, only a subset of the nucleoporins recognized by this antibody resides in NCSs: Nup153 and Nup62. Similarly, only some inner nuclear membrane (emerin) and lamina proteins (lamin A/C) are enriched in NCSs, whereas all tested proteins of the smooth endoplasmic reticulum are present. This selective composition of the NCS, together with its membrane tubules in the normally membrane-free nucleus, renders the NCS unique among nuclear organelles. Despite the analysis of only a sample of envelope proteins, it is clear that NCSs are not a mere extension but a specialization of the nuclear envelope.

Although membranous structures have been previously observed in nuclei, they were all artificially induced and differ in composition from the physiological NCSs as detailed below. R-rings, which are induced by exogenous expression of the nucleolar protein Nopp140, are virtually indistinguishable from NCSs at an ultrastructural level, hinting at a common derivation from the inner nuclear membrane (Isaac et al., 2001; Kittur et al., 2007). However, R-rings differ from NCSs in their composition, for example in their accumulation of nucleolar proteins that are absent from NCSs (Isaac et al., 2001; Kittur et al., 2007). Interestingly, overexpression of mammalian Nup153 and B-type lamins, which are both present in NCSs, and of the yeast Nup53 leads to intranuclear membrane formation (Bastos et al., 1996; Marelli et al., 2001; Prufert et al., 2004; Ralle et al., 2004). However, none of these proteins is overexpressed in NCS-positive cells because, unlike during their exogenous expression, nuclear envelope staining of these proteins is not increased compared with that of neighboring, NCS-free cells. Additionally, where available, these membranes differ in composition, because the Nup153-induced structures lack Nup62 and lamins (data not shown), and yeast Nup53 structures stain negative for mAb414 (Marelli et al., 2001). Moreover, membrane proliferation appeared to be dependent on the permanent farnesylation of B-type lamins (Prufert et al., 2004; Ralle et al., 2004), but this modification is removed from the more highly NCS enriched A-type lamins. Finally, the presence of lamins and only some nucleoporins sets NCSs apart from annulate lamellae, intact NPCs embedded in register in lamin-free stacks of smooth endoplasmic reticulum (Chen and Merisko, 1988). Consequently, NCSs are distinct from all these nuclear structures.

What causes the formation of NCSs? Apparently, NCSs are induced by the action of progesterone but steroid receptors are not enriched in NCSs (Table 2) (Kohorn et al., 1970; Kohorn et al., 1972; Pryse-Davies et al., 1979; Roberts et al., 1975). NCSs are only one of several precisely timed ultrastructural changes occurring in postovulation endometrial epithelial cells (Spornitz, 1992). The uniform 1 μm size of NCSs and the limited number of one per nucleus, indicate that their growth is controlled and not a random proliferation. Unlike in the artificial cases mentioned above, NCSs are not induced by simple overexpression of one of its components. This is supported by gene expression profiling studies of human endometrium, which report no upregulation of any of the NCS components identified here or of entire nuclear structures (Borthwick et al., 2003; Carson et al., 2002; Horcajadas et al., 2004; Kao et al., 2002; Mirkin et al., 2005; Riesewijk et al., 2003; Talbi et al., 2006). This is not surprising, considering that based on extrapolations of fluorescence intensity measurements to the surfaces of entire NCSs and nuclear envelopes, the amount in the NCS of its most prominent constituents (Nup153, emerin, and lamin A/C) equals that of the entire nuclear envelope. Therefore, the levels of those proteins need only increase twofold to account for their bright fluorescence in NCSs. In a tissue-wide analysis, this factor would be reduced by at least half owing to the presence of NCS-free epithelial cells. The signal would be further diluted by the large number of cells in each sample from the stromal compartment. Consequently, changes in messenger RNA abundance of these components would escape the sensitivity of a gene-profiling approach, arguing for more sensitive, single-cell-based assays, as reported here. In conclusion, the biogenesis of NCSs must be a finely balanced process.

Our molecular and physiological characterization of NCSs raises new questions as to their function(s). NCSs exhibit a three-component architecture, membrane tubules embedded in an electron-dense matrix, which together surround an amorphous core. Is one of these components the functionally important entity merely requiring the other two for its maintenance or are they required as a whole? Are NCSs sequestering specific molecules in their core? Based on the ring staining in sagittal NCS sections, we have only identified proteins of the NCS matrix and membranes but not its core. Are NCSs merely stockpiles of its individual components? The presence of only a subset of nuclear envelope components argues against a simple storage function. Is it possible that specific genes associate with NCSs, for activation or repression? Could the expression of such genes be important for communication of the epithelium with the blastocyst? Alternatively, could such genes

and/or the NCS be involved in inhibition of cell division because NCSs are only seen in cells whose proliferation has been halted by the action of progesterone (and not in cancer specimens)? What is the connection between the nucleolus and the NCS? The association/engulfment of half of NCSs with/by nucleoli suggests a functional link. Is this link related to the major function of nucleoli, ribosome biogenesis, or to one of their many, more recently identified activities (Boisvert et al., 2007)? Using the simple NCS detection method and molecular dissection herein described will allow investigators to approach these and other questions. The importance of our discovery of an NCS marker is perhaps best illustrated by the remarkable insight gained into the function of Cajal bodies – other nuclear bodies known for over 100 years – since the identification of their marker coilin (Gall, 2003; Raska et al., 1991).

Materials and Methods

Human endometrial biopsies

Endometrial biopsies were obtained by informed consent from normally cycling women at two sites, Albert Einstein College of Medicine, Bronx, NY (site 1, 50 biopsies) and University of North Carolina School of Medicine, Chapel Hill, NC (site 2, 45 biopsies). The respective Institutional Review Boards approved the collection protocols. The site 1 protocol was described previously (Kittur et al., 2007). Endometrial tissue was fixed with 4% paraformaldehyde in phosphate-buffered saline. Routine histological methods were used for paraffin embedding and sectioning of tissue. A total of 28 hematoxylin and eosin stained sections of site 1 biopsies were scored blinded for the cycle day by two independent histopathologists using classical criteria (Noyes et al., 1950). The site 2 protocol was identical, except that all samples were obtained from normal volunteers and cycle timing was based on cycle day (proliferative) and urine LH surge identification (secretory). Cycle day was confirmed by a single investigator blinded to LH data using the same criteria of Noyes (Noyes et al., 1950). No biopsies were reassigned to a different cycle day based on histological review.

Immunostaining of tissue sections

For immunostaining, sections on slides were first deparaffinized by heating at 60°C for 20 minutes, and rehydrated as follows: twice in xylene (5 minutes each), 100% ethanol (10 minutes), 95% ethanol (5 minutes), 80% ethanol (2 minutes), 70% ethanol (2 minutes), twice in distilled water (2 minutes each). For subsequent antigen retrieval, slides were microwave-heated at full power (2 minutes) in 10 mM sodium citrate (pH 6.0) and steamed in a rice cooker (20 minutes). After cooling to room temperature, slides were rinsed with phosphate-buffered saline and processed for routine immunostaining as described, except that the sections were not further permeabilized with detergent (Isaac et al., 1998).

Cryosectioning was performed by the method of Tokuyasu as described previously (Kittur et al., 2007). For light microscopy, 0.5-μm-thick (semi-thin) cryosections were cut from the fixed tissue, picked up using 2.3 M sucrose and placed on glass coverslips. The sucrose was dissolved by incubating the sections in nanopure water. Sections were next permeabilized by the following treatment for 30 seconds each: xylene, 100% ethanol, 95% ethanol, 80% ethanol, 70% ethanol and distilled water. The antigen retrieval and immunostaining was identical to that described above for the paraffin sections.

Tissue arrays used were 59 endometrial carcinomas (adenocarcinomas grade I-III) (Cybrdi, Frederick, MD), normal tissue of multiple organs from 48 patients (Cybrdi), and 59 normal endometrial sections (Imgenex, San Diego, CA). Tissue cores on the array slides were formalin-fixed and processed for immunostaining as described above. Sections of secretory endometrium from 19 baboons were kindly provided by Asgi Fazleabas, University of Illinois, Chicago.

Antibodies

Mouse IgGs (Covance Research Products, Princeton, NJ) of mAb414 (Davis and Blobel, 1986) were used at 2 μg/ml for light and at 500 μg/ml for electron microscopy. The following primary antibodies were used on paraffin and cryosections at the dilutions indicated in parentheses: anti-calnexin rabbit polyclonal serum (SPA860 at 1:200; Assay Designs/StressGen, Ann Arbor, MI), anti-BiP mouse IgGs (10C3 anti-KDEL at 2.5 μg/ml, Assay Designs/StressGen); anti-PDI polyclonal serum (SPA860 at 1:200, Assay Designs/StressGen); anti-Sec61β rabbit serum (1:200 using RNase) (Fons et al., 2003; Snapp et al., 2004); anti-human Nopp140 rabbit polyclonal serum (RS8 1:500) (Kittur et al., 2007); anti-human NAP57 rabbit polyclonal serum (RU8 at 1:200) (Darzacq et al., 2006); anti-fibrillarin mouse monoclonal IgG (clone D77 at 1 μg/ml) (Aris and Blobel, 1988); anti-nucleolin mouse ascites fluid (clone 7G2 at 1:1000) (Pinol-Roma, 1999); anti-UBF1 rabbit polyclonal serum (1:100, from Larry Rothblum, University of Oklahoma Medical College, Oklahoma City, OK); anti-SC35 mouse ascites fluid (1:1000, Sigma, St Louis, MO); anti-coilin mouse ascites fluid (clone 5P10 at 1:1000) (Almeida et al., 1998); anti-RNA polymerase II C-terminal domain mouse monoclonal culture supernatants (clone H14, IgM undiluted, initiating) and (clone H5, IgG undiluted, elongating) (Bregman et al., 1995); anti-Nup153 mouse monoclonal ascites fluid (clone 322 at 1:100) (Sukegawa and Blobel, 1993) and culture supernatant (clone SA1 at 1:10) (Bodoor et al., 1999); anti-Nup358 rabbit polyclonal serum (1:500) (Wu et al., 1995); anti-Tpr rabbit polyclonal serum (Tpr C at 1:300) (Frosst et al., 2002); anti-Nup62 goat polyclonal serum (sc-1916 at 1:20, Santa Cruz Biotechnology, Santa Cruz, CA); anti-Nup214 rabbit polyclonal serum (1:50, from Joseph Glavy, Stevens Institute of Technology, Hoboken, NJ); anti-lamin A/C rabbit polyclonal IgG (sc-20681 at 2 μg/ml, Santa Cruz Biotechnology); anti-lamin A goat polyclonal IgG (sc-6214 at 4 μg/ml, Santa Cruz Biotechnology); anti-lamin B1 rabbit polyclonal serum (1:1000) (Moss et al., 1999); anti-lamin B2 mouse monoclonal IgG (clone LN43 at 100 μg/ml, Chemicon, Temecula, CA); anti-LAP2β mouse monoclonal IgG (5 μg/ml, BD Transduction Laboratories, San Diego, CA); anti-emerin mouse monoclonal culture supernatant (clone 4G5 at 1:20, Novocastra Laboratories, Newcastle upon Tyne, UK); anti-CLIMP63 rabbit polyclonal serum (1:200) (Schweizer et al., 1995); anti-p115 rabbit polyclonal serum (1:500) (Mukherjee et al., 2007); anti-GM130 mouse monoclonal IgG (clone 35 at 1.25 μg/ml, BD Transduction Laboratories); anti-progesterone receptor rabbit polyclonal IgG (sc-538 at 2 μg/ml, Santa Cruz Biotechnology, and ab15509 at 2 μg/ml, Abcam, Cambridge, MA); anti-estrogen receptor α rabbit polyclonal IgG (sc-542 at 2 μg/ml, Santa Cruz Biotechnology); Fluorescently labeled wheat germ agglutinin (WGA at 0.1 mg/ml, Sigma). Note that although all antibodies stained cells in their predicted pattern, we cannot rule out that the lack of NCS staining in some cases could result from masking or loss of an epitope specifically in NCSs.

DNA was stained with 4′, 6-diaminidino-2-phenylindole dihydrochloride (DAPI at 1 μg/ml, Sigma). Secondary antibodies for immunofluorescence against IgGs were Cy3 or Cy5 conjugated donkey anti-mouse, Cy2-conjugated donkey anti-rabbit, and Cy3-conjugated donkey anti-goat (1:200, Jackson ImmunoResearch, West Grove, PA), and Alexa Fluor 488-conjugated goat anti-mouse IgMs (1:200, Invitrogen, Carlsbad, CA).

Imaging

All imaging was done at the Analytical Imaging Facility of the Albert Einstein College of Medicine. Epifluorescence of cryosections and paraffin sections was performed with the identical procedure and equipment as described recently (Kittur et al., 2007). Confocal laser-scanning microscopy of paraffin sections was performed on an SP2 AOBS microscope (Leica, Mannheim, Germany) using a 63×/1.4 NA planapo objective. Image stacks were reconstructed in three-dimensions, enhanced, and analyzed using ImageJ software (National Institutes of Health, Bethesda, MD).

NCS quantification

Quantification of NCSs using mAb414 on paraffin sections was first established on a three-dimensional training set of 11 endometrial specimens from luteal days 4-11 (Table 1). For this purpose, the ~7-μm-thick sections were imaged with the confocal laser-scanning microscope at 0.2 μm steps. In order to account for all NCSs, maximum projections of all stacks were reconstructed using the standard deviation method of ImageJ software (e.g. Fig. 1C'). Between 237 and 1305 epithelial cell nuclei for each biopsy were visually inspected for NCSs. The numbers from this analysis were related to those observed by two-dimensional analysis of the same biopsies using epifluorescence. In this manner, biopsies were classified into three categories, those without NCSs (0%), those with low amounts (<10%) and those with plenty of NCSs, most commonly around 50% (~50%). All residual biopsies were analyzed using epifluorescence and assigned to one of these three categories. All analysis and scoring was done independently by at least two observers who were blinded as to the cycle day.

We thank Asgi Fazleabas for providing paraffin sections of secretory baboon endometria. For providing the referenced antibodies, we are grateful to John Aris, Brian Burke, Nilabh Chaudhary, Maria Carmo Fonseca, Joe Glavy, Serafin Pinol-Roma, Jack Rohrer, Larry Rothblum, Yaron Shav-Tal, Dennis Shields and Erik Snapp. We acknowledge Amy Brown and Gail Grossman for recruitment of site 2 subjects and processing of specimens. We appreciate the services and use of the Analytical Imaging and of the Histotechnology and Comparative Pathology Facilities of the Albert Einstein College of Medicine. This work was supported by grants from the March of Dimes Birth Defects Foundation (1-FY05-125) to U.T.M. and the National Institutes of Health (2U54HD035041-11) to S.L.Y. E.G. and N.K. did all experiments. Z.N.B. performed tissue array analyses. A.J.P. and S.M.K. collected site 1 biopsies. N.S. coordinated biopsy collection and, together with D.S.H., histologically dated biopsies. S.L.Y. provided all site two biopsies. U.T.M. conceived and directed the study, and wrote the manuscript.

References

Acosta, A. A., Elberger, L., Borghi, M., Calamera, J. C., Chemes, H., Doncel, G. F., Kliman, H., Lema, B., Lustig, L. and Papier, S. (2000). Endometrial dating and determination of the window of implantation in healthy fertile women. *Fertil. Steril.* **73**, 788-798.

Aghajanova, L., Hamilton, A. E. and Giudice, L. C. (2007). Uterine receptivity to human embryonic implantation: histology, biomarkers, and transcriptomics. *Semin. Cell Dev. Biol.* **19**, 204-211.

Almeida, F., Saffrich, R., Ansorge, W. and Carmo-Fonseca, M. (1998). Microinjection of anti-coilin antibodies affects the structure of coiled bodies. *J. Cell Biol.* **142**, 899-912.

Aris, J. and Blobel, G. (1988). Identification and characterization of a yeast nucleolar protein that is similar to a rat liver nucleolar protein. *J. Cell Biol.* **107**, 17-31.

Azadian-Boulanger, G., Secchi, J., Laraque, F., Raynaud, J. P. and Sakiz, E. (1976). Action of midcycle contraceptive (R 2323) on the human endometrium. *Am. J. Obstet. Gynecol.* **125**, 1049-1056.

Bastos, R., Lin, A., Enarson, M. and Burke, B. (1996). Targeting and function in mRNA export of nuclear pore complex protein Nup153. *J. Cell Biol.* **134**, 1141-1156.

Belgareh, N., Rabut, G., Bai, S. W., van Overbeek, M., Beaudouin, J., Daigle, N., Zatsepina, O. V., Pasteau, F., Labas, V., Fromont-Racine, M. et al. (2001). An evolutionarily conserved NPC subcomplex, which redistributes in part to kinetochores in mammalian cells. *J. Cell Biol.* **154**, 1147-1160.

Bentin-Ley, U., Sjogren, A., Nilsson, L., Hamberger, L., Larsen, J. F. and Horn, T. (1999). Presence of uterine pinopodes at the embryo-endometrial interface during human implantation in vitro. *Hum. Reprod.* **14**, 515-520.

Bodoor, K., Shaikh, S., Salina, D., Raharjo, W. H., Bastos, R., Lohka, M. and Burke, B. (1999). Sequential recruitment of NPC proteins to the nuclear periphery at the end of mitosis. *J. Cell Sci.* **112**, 2253-2264.

Boisvert, F. M., van Koningsbruggen, S., Navascues, J. and Lamond, A. I. (2007). The multifunctional nucleolus. *Nat. Rev. Mol. Cell Biol.* **8**, 574-585.

Borthwick, J. M., Charnock-Jones, D. S., Tom, B. D., Hull, M. L., Teirney, R., Phillips, S. C. and Smith, S. K. (2003). Determination of the transcript profile of human endometrium. *Mol. Hum. Reprod.* **9**, 19-33.

Bregman, D. B., Du, L., van der Zee, S. and Warren, S. L. (1995). Transcription-dependent redistribution of the large subunit of RNA polymerase II to discrete nuclear domains. *J. Cell Biol.* **129**, 287-298.

Carson, D. D., Lagow, E., Thathiah, A., Al-Shami, R., Farach-Carson, M. C., Vernon, M., Yuan, L., Fritz, M. A. and Lessey, B. (2002). Changes in gene expression during the early to mid-luteal (receptive phase) transition in human endometrium detected by high-density microarray screening. *Mol. Hum. Reprod.* **8**, 871-879.

Chen, T. Y. and Merisko, E. M. (1988). Annulate lamellae: comparison of antigenic epitopes of annulate lamellae membranes with the nuclear envelope. *J. Cell Biol.* **107**, 1299-1306.

Clyman, M. J. (1963). A new structure observed in the nucleolus of the human endometrial epithelial cell. *Am. J. Obstet. Gynecol.* **86**, 430-432.

Coutifaris, C., Myers, E. R., Guzick, D. S., Diamond, M. P., Carson, S. A., Legro, R. S., McGovern, P. G., Schlaff, W. D., Carr, B. R., Steinkampf, M. P. et al. (2004). Histological dating of timed endometrial biopsy tissue is not related to fertility status. *Fertil. Steril.* **82**, 1264-1272.

Darzacq, X., Kittur, N., Roy, S., Shav-Tal, Y., Singer, R. H. and Meier, U. T. (2006). Stepwise RNP assembly at the site of H/ACA RNA transcription in human cells. *J. Cell Biol.* **173**, 207-218.

Davis, L. I. and Blobel, G. (1986). Identification and characterization of a nuclear pore complex protein. *Cell* **45**, 699-709.

Davis, L. I. and Blobel, G. (1987). Nuclear pore complex contains a family of glycoproteins that includes p62: glycosylation through a previously unidentified cellular pathway. *Proc. Natl. Acad. Sci. USA* **84**, 7552-7556.

de los Santos, M. J., Mercader, A., Galan, A., Albert, C., Romero, J. L. and Pellicer, A. (2003). Implantation rates after two, three, or five days of embryo culture. *Placenta* **24** Suppl. B, S13-S19.

Dockery, P., Pritchard, K., Warren, M. A., Li, T. C. and Cooke, I. D. (1996). Changes in nuclear morphology in the human endometrial glandular epithelium in women with unexplained infertility. *Hum. Reprod.* **11**, 2251-2256.

Dubrauszky, V. and Pohlmann, G. (1960). Strukturveränderungen am Nukleolus von Korpusendometriumzellen während der Sekretionsphase. *Naturwissenschaften* **47**, 523-524.

Feria-Velasco, A., Aznar-Ramos, R. and Gonzalez-Angulo, A. (1972). Ultrastructural changes found in the endometrium of women using megestrol acetate for contraception. *Contraception* **5**, 187-201.

Fons, R. D., Bogert, B. A. and Hegde, R. S. (2003). Substrate-specific function of the translocon-associated protein complex during translocation across the ER membrane. *J. Cell Biol.* **160**, 529-539.

Frosst, P., Guan, T., Subauste, C., Hahn, K. and Gerace, L. (2002). Tpr is localized within the nuclear basket of the pore complex and has a role in nuclear protein export. *J. Cell Biol.* **156**, 617-630.

Gall, J. G. (2003). The centennial of the Cajal body. *Nat. Rev. Mol. Cell Biol.* **4**, 975-980.

Gore, B. Z. and Gordon, M. (1974). Fine structure of epithelial cell of secretory endometrium in unexplained primary infertility. *Fertil. Steril.* **25**, 103-107.

Hase, M. E. and Cordes, V. C. (2003). Direct interaction with Nup153 mediates binding of Tpr to the periphery of the nuclear pore complex. *Mol. Biol. Cell* **14**, 1923-1940.

Horcajadas, J. A., Riesewijk, A., Martin, J., Cervero, A., Mosselman, S., Pellicer, A. and Simon, C. (2004). Global gene expression profiling of human endometrial receptivity. *J. Reprod. Immunol.* **63**, 41-49.

Isaac, C., Yang, Y. and Meier, U. T. (1998). Nopp140 functions as a molecular link between the nucleolus and the coiled bodies. *J. Cell Biol.* **142**, 319-329.

Isaac, C., Pollard, J. W. and Meier, U. T. (2001). Intranuclear endoplasmic reticulum induced by Nopp140 mimics the nucleolar channel system of human endometrium. *J. Cell Sci.* **114**, 4253-4264.

Kao, L. C., Tulac, S., Lobo, S., Imani, B., Yang, J. P., Germeyer, A., Osteen, K., Taylor, R. N., Lessey, B. A. and Giudice, L. C. (2002). Global gene profiling in human endometrium during the window of implantation. *Endocrinology* **143**, 2119-2138.

Kittur, N., Zapantis, G., Aubuchon, M., Santoro, N., Bazett-Jones, D. P. and Meier, U. T. (2007). The Nucleolar channel system of human endometrium is related to endoplasmic reticulum and R-rings. *Mol. Biol. Cell* **18**, 2296-2304.

Klopfenstein, D. R., Klumperman, J., Lustig, A., Kammerer, R. A., Oorschot, V. and Hauri, H. P. (2001). Subdomain-specific localization of CLIMP-63 (p63) in the endoplasmic reticulum is mediated by its luminal alpha-helical segment. *J. Cell Biol.* **153**, 1287-1300.

Kohorn, E. I., Rice, S. I. and Gordon, M. (1970). In vitro production of nucleolar channel system by progesterone in human endometrium. *Nature* **228**, 671-672.

Kohorn, E. I., Rice, S. I., Hemperly, S. and Gordon, M. (1972). The relation of the structure of progestational steroids to nucleolar differentiation in human endometrium. *J. Clin. Endocrinol. Metab.* **34**, 257-264.

Krull, S., Thyberg, J., Bjorkroth, B., Rackwitz, H. R. and Cordes, V. C. (2004). Nucleoporins as components of the nuclear pore complex core structure and Tpr as the architectural element of the nuclear basket. *Mol. Biol. Cell* **15**, 4261-4277.

Lin, F., Blake, D. L., Callebaut, I., Skerjanc, I. S., Holmer, L., McBurney, M. W., Paulin-Levasseur, M. and Worman, H. J. (2000). MAN1, an inner nuclear membrane protein that shares the LEM domain with lamina-associated polypeptide 2 and emerin. *J. Biol. Chem.* **275**, 4840-4847.

MacLennan, A. H., Harris, J. A. and Wynn, R. M. (1971). Menstrual cycle of the baboon. II. Endometrial ultrastructure. *Obstet. Gynecol.* **38**, 359-374.

Marelli, M., Lusk, C. P., Chan, H., Aitchison, J. D. and Wozniak, R. W. (2001). A Link between the synthesis of nucleoporins and the biogenesis of the nuclear envelope. *J. Cell Biol.* **153**, 709-724.

Martel, D. (1981). Surface changes of the luminal uterine epithelium during the human menstrual cycle, a scanning microscopic study. In *The Endometrium: Hormonal Implants* (ed J. Brux and J. P. Gantry), pp. 15-29. New York: Plenum.

Mirkin, S., Arslan, M., Churikov, D., Corica, A., Diaz, J. I., Williams, S., Bocca, S. and Oehninger, S. (2005). In search of candidate genes critically expressed in the human endometrium during the window of implantation. *Hum. Reprod.* **20**, 2104-2117.

Moricard, R. and Moricard, F. (1964). Modifications cytoplasmiques et nucléaires ultrastructurales utérines au cours de l'état follico-lutéinique à glycogène massif. *Gynecol. Obstet.* **63**, 203-219.

Moss, S. F., Krivosheyev, V., de Souza, A., Chin, K., Gaetz, H. P., Chaudhary, N., Worman, H. J. and Holt, P. R. (1999). Decreased and aberrant nuclear lamin expression in gastrointestinal tract neoplasms. *Gut* **45**, 723-729.

Mukherjee, S., Chiu, R., Leung, S. M. and Shields, D. (2007). Fragmentation of the Golgi apparatus: an early apoptotic event independent of the cytoskeleton. *Traffic* **8**, 369-378.

Murray, M. J., Meyer, W. R., Zaino, R. J., Lessey, B. A., Novotny, D. B., Ireland, K., Zeng, D. and Fritz, M. A. (2004). A critical analysis of the accuracy, reproducibility, and clinical utility of histologic endometrial dating in fertile women. *Fertil. Steril.* **81**, 1333-1343.

Nikas, G., Drakakis, P., Loutradis, D., Mara-Skoufari, C., Koumantakis, E., Michalas, S. and Psychoyos, A. (1995). Uterine pinopodes as markers of the 'nidation window' in cycling women receiving exogenous oestradiol and progesterone. *Hum. Reprod.* **10**, 1208-1213.

Norwitz, E. R., Schust, D. J. and Fisher, S. J. (2001). Implantation and the survival of early pregnancy. *N. Engl. J. Med.* **345**, 1400-1408.

Novotny, R., Malinsky, J., Oborna, I. and Dostal, J. (1999). Nuclear channel system (NCS) in normal endometrium and after hormonal stimulation. *Acta Univ. Palacki. Olomuc. Fac. Med.* **142**, 41-46.

Noyes, R. W., Hertig, A. I. and Rock, J. (1950). Dating the endometrial biopsy. *Fertil. Steril.* **1**, 3-25.

Petersen, A., Bentin-Ley, U., Ravn, V., Qvortrup, K., Sorensen, S., Islin, H., Sjogren, A., Mosselmann, S. and Hamberger, L. (2005). The antiprogesterone Org 31710 inhibits human blastocyst-endometrial interactions in vitro. *Fertil. Steril.* **83** Suppl. 1, 1255-1263.

Pinol-Roma, S. (1999). Association of nonribosomal nucleolar proteins in ribonucleoprotein complexes during interphase and mitosis. *Mol. Biol. Cell* **10**, 77-90.

Prufert, K., Vogel, A. and Krohne, G. (2004). The lamin CxxM motif promotes nuclear membrane growth. *J. Cell Sci.* **117**, 6105-6116.

Pryse-Davies, J., Ryder, T. A. and MacKenzie, M. L. (1979). In vivo production of the nucleolar channel system in post menopausal endometrium. *Cell Tissue Res.* **203**, 493-498.

Quinn, C., Ryan, E., Claessens, E. A., Greenblatt, E., Hawrylyshyn, P., Cruickshank, B., Hannam, T., Dunk, C. and Casper, R. F. (2007). The presence of pinopodes in the human endometrium does not delineate the implantation window. *Fertil. Steril.* **87**, 1015-1021.

Rabut, G., Doye, V. and Ellenberg, J. (2004). Mapping the dynamic organization of the nuclear pore complex inside single living cells. *Nat. Cell Biol.* **6**, 1114-1121.

Ralle, T., Grund, C., Franke, W. W. and Stick, R. (2004). Intranuclear membrane structure formations by CaaX-containing nuclear proteins. *J. Cell Sci.* **117**, 6095-6104.

Raska, I., Andrade, L. E. C., Ochs, R. L., Chan, E. K. L., Chang, C.-M., Roos, G. and Tan, E. M. (1991). Immunological and ultrastructural studies of the nuclear coiled body with autoimmune antibodies. *Exp. Cell Res.* **195**, 27-37.

Riesewijk, A., Martin, J., van Os, R., Horcajadas, J. A., Polman, J., Pellicer, A., Mosselman, S. and Simon, C. (2003). Gene expression profiling of human endometrial receptivity on days LH+2 versus LH+7 by microarray technology. *Mol. Hum. Reprod.* **9**, 253-264.

Roberts, D. K., Horbelt, D. V. and Powell, L. C., Jr (1975). The ultrastructural response of human endometrium to medroxyprogesterone acetate. *Am. J. Obstet. Gynecol.* **123**, 811-818.

Ryder, T. A., Mobberley, M. A. and Whitehead, M. I. (1995). The endometrial nucleolar channel system as an indicator of progestin potency in HRT. *Maturitas* **22**, 31-36.

Schweizer, A., Rohrer, J., Slot, J. W., Geuze, H. J. and Kornfeld, S. (1995). Reassessment of the subcellular localization of p63. *J. Cell Sci.* **108**, 2477-2485.

Snapp, E. L., Reinhart, G. A., Bogert, B. A., Lippincott-Schwartz, J. and Hegde, R. S. (2004). The organization of engaged and quiescent translocons in the endoplasmic reticulum of mammalian cells. *J. Cell Biol.* **164**, 997-1007.

Spornitz, U. M. (1992). The functional morphology of the human endometrium and decidua. *Adv. Anat. Embryol. Cell Biol.* **124**, 1-99.

Stewart, C. L., Roux, K. J. and Burke, B. (2007). Blurring the boundary: the nuclear envelope extends its reach. *Science* **318**, 1408-1412.

Sukegawa, J. and Blobel, G. (1993). A nuclear pore complex protein that contains zinc finger motifs, binds DNA, and faces the nucleoplasm. *Cell* **72**, 29-38.

Talbi, S., Hamilton, A. E., Vo, K. C., Tulac, S., Overgaard, M. T., Dosiou, C., Le Shay, N., Nezhat, C. N., Kempson, R., Lessey, B. A. et al. (2006). Molecular phenotyping of human endometrium distinguishes menstrual cycle phases and underlying biological processes in normo-ovulatory women. *Endocrinology* **147**, 1097-10121.

Terry, L. J., Shows, E. B. and Wente, S. R. (2007). Crossing the nuclear envelope: hierarchical regulation of nucleocytoplasmic transport. *Science* **318**, 1412-1416.

Terzakis, J. A. (1965). The nucleolar channel system of the human endometrium. *J. Cell Biol.* **27**, 293-304.

Tran, E. J. and Wente, S. R. (2006). Dynamic nuclear pore complexes: life on the edge. *Cell* **125**, 1041-1053.

Trinkle-Mulcahy, L. and Lamond, A. I. (2007). Toward a high-resolution view of nuclear dynamics. *Science* **318**, 1402-1407.

Usadi, R. S., Murray, M. J., Bagnell, R. C., Fritz, M. A., Kowalik, A. I., Meyer, W. R. and Lessey, B. A. (2003). Temporal and morphologic characteristics of pinopod expression across the secretory phase of the endometrial cycle in normally cycling women with proven fertility. *Fertil. Steril.* **79**, 970-974.

Wagner, N. and Krohne, G. (2007). LEM-Domain proteins: new insights into lamin-interacting proteins. *Int. Rev. Cytol.* **261**, 1-46.

Wilcox, A. J., Baird, D. D. and Weinberg, C. R. (1999). Time of implantation of the conceptus and loss of pregnancy. *N. Engl. J. Med.* **340**, 1796-1799.

Wu, J., Matunis, M. J., Kraemer, D., Blobel, G. and Coutavas, E. (1995). Nup358, a cytoplasmically exposed nucleoporin with peptide repeats, Ran-GTP binding sites, zinc fingers, a cyclophilin A homologous domain, and a leucine-rich region. *J. Biol. Chem.* **270**, 14209-14213.

Wynn, R. M. (1967). Intrauterine devices: effects on ultrastructure of human endometrium. *Science* **156**, 1508-1510.

Journal of Cell Science